ISSN (Print) 1226-1750
ISSN (Online) 2233-6656
Journal of Magnetics 24(4), 688-697 (2019) https://doi.org/10.4283/JMAG.2019.24.4.688

Investigation of Convective Heat and Mass Conditions in Squeeze Flow of a Hydro-magnetic Sutterby Fluid

S. Ahmad[1]*, M. Farooq[1], Aisha Anjum[1], and Samreen Sheriff[1,2]

[1]*Department of Mathematics and Statistics, Riphah International University, Islamabad 44000, Pakistan*
[2]*DBS&H, CEME, National University of Sciences and Technology, Islamabad 44000, Pakistan*

(Received 13 January 2019, Received in final form 14 November 2019, Accepted 16 November 2019)

Analysis regarding convective surface phenomenon has emerged to be effective approach to depict refinements in thermal features, since most of the heat/mass transfer surfaces are disclosed to a convective environment at specified parameters which cannot be achieved through energy analysis. The development in the dynamics of convective heat and mass transport is significant in understanding diverse engineering and industrial phenomena such as in thermal energy storage material drying process, transpiration cooling process, and many others. Keeping aforementioned usefulness in mind, the current analysis is aimed to demonstrate the convective features in squeezed Sutterby fluid flow through parallel surfaces. Magneto-hydrodynamic (MHD) theory is incorporated to describe the squeezing flow phenomenon. The Sutterby fluid model is accounted in order to specify the flow nature in squeezed channel. The top plate is assumed to be squeezed whereas the lower plate is at rest. The convective heating is incorporated at both lower and upper plates. Inspection of mass transfer has been accomplished in the occupancy of solutal convective conditions at the both surfaces. The equations governing the flow, heat and mass transport are first derived under the assumptions of low magnetic Reynolds number and negligible viscous dissipation, and then made non-dimensional by defining the similarity variables. Series solutions representing the flow velocity, temperature and concentration distributions are computed for definite values of power law index by utilizing convergent approach. Results are graphed and physical elucidated is seen for involved flow parameters. Variations in co-efficient of skin friction, Nusselt and Sherwood numbers are reported graphically. Significant findings in this attempt is that higher lower plate thermal and solutal Biot numbers strengthen the both heat and mass fluxes, while larger upper plate thermal and solutal Biot numbers weaken the heat and mass fluxes.

Keywords : squeezing flow, sutterby fluid, magneto-hydrodynamic, convective heat and mass fluxes

1. Introduction

Different kinds of fluids having different properties are encountered in many industrial and manufacturing processes such as organic chain mixtures, polymer melts, colloidal suspensions etc. Rheological attributes of such fluids are not entirely described by Naiver-Stokes equations. Consequently, to understand the rheological attributes of complex fluids, several non-linear fluid models have suggested. The fluid model [1] named after Sutterby includes in the category of fluid models which are non-Newtonian in character. It is utilized to scrutinize the notable characteristics of pseudo-plastic and dilatant liquids. This model has advantage over other flow models to exhibit fluid behavior as Newtonian, shear thinning and thickening fluids for diverse values of unit free power law index *n*. Akbar and Nadeem [2] exposed the convectively heated Sutterby fluid flow in asymmetric channel considering velocity slip. Blood flow assessment for Sutterby fluid into stenosed arteries is exhibited by Akbar [3]. Hayat *et al.* [4] constructed the peristaltic motion of radiative Sutterby fluid in vertical channel yield compliant wall characteristics. Hayat *et al*. [5] addressed the radiative heat transfer in peristalsis of Sutterby liquid flow through curved channel with Joule heating. Flow behavior of Sutterby nanofluid in stagnation region characterized via entropy generation is depicted by Azhar *et al*. [6]. Hayat *et al*. [7] studied the wall radiative properties in peristaltic motion of hydro-magneto Sutterby fluid embedded in curved channel. Hayat *et al*. [8] dislodged the development

*Corresponding author: Tel: +923335377399
e-mail: shakeel_oiiui@yahoo.com

in the Sutterby type fluid flow through Darcy-Forchheimer medium under peristaltic mechanism. Shankar and Naduvinamani [9] explored the squeezing magnetized flow of Casson fluid under generalized diffusive theory. Hayat *et al*. [10] addressed the melting phenomenon in squeezed third-garde fluid flow by implementing modified heat flux. Few more investigations involving non-Newtonian fluids can be mentioned through refs. [11, 12].

Transport mechanism of heat and mass is widely used to analyze the characteristics of such fluids which are non-Newtonian in character. These mechanism have a favorable usage in numerous built-up and trade areas, for instance, metallurgical process, glass blowing, polymer extrusion, combustion systems, in chemical engineering and other advances. In such transport activities, buoyancy forces affect the thermal and mass diffusion processes that were occurred in cooling and heating chambers, solar power technology, space technology and energy processes etc. Recently some attempts are disclosed the heat and mass transport procedure in flow with convective temperature and concentration surface conditions. Eegunjobi and Makinde [13] disclosed the irreversibility analysis in convectively heated hydro-magnetic flow through porous walls with varying viscosity. Shahzad *et al*. [14] illustrated the MHD flow of nanofluid characterized via convective temperature and concentration conditions. Hayat *et al*. [15] discussed the convectively heated and concentrated Powell-Eyring fluid flow onto a sheet which is stretched exponentially. Ashraf *et al*. [16] exhibited the influence of convective type conditions at boundary on MHD flow of radiative Jeffrey nanomaterial past a stretched sheet with mixed convection. Das *et al*. [17] disclosed the flow phenomenon of MHD second grade fluid past through convectively heated and concentrated stretchable surface. Pushpalatha *et al*. [18] reflected the magneto Casson liquid flow considering convective surface conditions. The impact of convective conditions on squeezed liquid flow over a Riga sheet with aspects of chemical reaction is disclosed by Hayat *et al*. [19]. Khan *et al*. [20] explored the effect of convective surface conditions on Carreau nanofluid flow over stretchable surface. Farooq *et al*. [21] disclosed the chemically reactive flow of squeezed fluid through generalized diffusive models. Ullah *et al*. [22] exposed the radiative features in chemically reactive magneto squeezed nanofluid flow through parallel disks. Some other attempts have been made to examine heat transfer in squeeze flows through refs. [23, 24].

The desire of current attempt is to address the MHD squeezing flow of Sutterby fluid between parallel plates. Heat and mass transfer involves convective boundary conditions. The current study mainly focused on exploring the effects of thermal and solutal Biot numbers onto both lower and upper walls. Convergent series solutions are derived for the resulting nonlinear analysis via homotopy technique (HAM) [25-34]. The impact of involved countless variables are graphically constructed. Graphical outcomes for skin friction (drag force), Nusselt and Sherwood numbers are also portrayed and conferred. Moreover the present paper is organized in such way that the flow equations are developed mathematically with appropriate assumptions in Section 2. Series solutions and their convergence description are obtained in Section 3 and Section 4 documents the results and interpretation. Also Section 5 compiles the main observation of the paper.

2. Problem Formulation

We consider an electrically conducted squeezed Sutterby fluid flow through two horizontal sheets. Let $h(t)$ be the minimum gap width between the sheets. The flow between the plates is developed due to the motion of top plate with vertical velocity $-(\gamma/2)\sqrt{\nu/a(1-\gamma t)}$ towards the bottom plate fixed at $y = 0$ which set into motion in its own plane with stretching velocity $ax/(1-\gamma t)$. A Cartesian coordinate system (x, y), in which axes x and y are normal to each other is used (See Fig. 1). Let u and v be the components of velocity in x and y directions respectively. The flow between the two plates is assumed to be unsteady and incompressible. A constant strength of magnetic field $B_0/\sqrt{1-\gamma t}$ is utilized in y-direction. A small Reynolds number (magnetic) is assumed in order to ignore the induced magnetic field. It is assumed that both lower and upper plates are convectively heated and concentrated which are influenced on heat and mass transport characteristics. Under the aforementioned assumptions, the mass, momentum, energy and diffusion equations become [6] & [27]:

$$\frac{\partial u}{\partial x}+\frac{\partial v}{\partial y}=0, \tag{2.1}$$

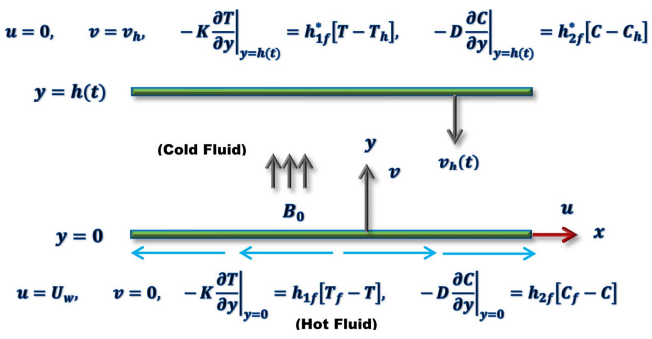

Fig. 1. (Color online) Flow geometry.

$$\frac{\partial u}{\partial t}+u\frac{\partial u}{\partial x}+v\frac{\partial u}{\partial y}=-\frac{1}{\rho}\frac{\partial p}{\partial x}+\nu\left(1-\frac{B^2}{6}\left(4\left(\frac{\partial u}{\partial x}\right)^2+\left(\frac{\partial u}{\partial y}+\frac{\partial v}{\partial x}\right)^2\right)\right)^n\left(2\frac{\partial^2 u}{\partial x^2}+\frac{\partial^2 u}{\partial y^2}+\frac{\partial^2 v}{\partial x\partial y}\right)$$
$$-\frac{2n\nu B^2}{6}\left(1-\frac{B^2}{6}\left(4\left(\frac{\partial u}{\partial x}\right)^2+\left(\frac{\partial u}{\partial y}+\frac{\partial v}{\partial x}\right)^2\right)\right)^{n-1}$$
$$\left(8\left(\frac{\partial u}{\partial x}\right)^2\frac{\partial^2 u}{\partial x^2}+2\frac{\partial u}{\partial x}\left(\frac{\partial u}{\partial y}+\frac{\partial v}{\partial x}\right)\left(\frac{\partial^2 u}{\partial x\partial y}+\frac{\partial^2 v}{\partial x^2}\right)\right) \quad (2.2)$$
$$-\frac{n\nu B^2}{6}\left(1-\frac{B^2}{6}\left(4\left(\frac{\partial u}{\partial x}\right)^2+\left(\frac{\partial u}{\partial y}+\frac{\partial v}{\partial x}\right)^2\right)\right)^{n-1}$$
$$\left(8\frac{\partial u}{\partial x}\frac{\partial^2 u}{\partial x\partial y}\left(\frac{\partial u}{\partial y}+\frac{\partial v}{\partial x}\right)+2\frac{\partial u}{\partial x}\left(\frac{\partial u}{\partial y}+\frac{\partial v}{\partial x}\right)^2\left(\frac{\partial^2 u}{\partial y^2}+\frac{\partial^2 v}{\partial x\partial y}\right)\right)-\frac{\sigma B_0^2}{\rho(1-\gamma t)}u,$$

$$\frac{\partial v}{\partial t}+u\frac{\partial v}{\partial x}+v\frac{\partial v}{\partial y}=-\frac{1}{\rho}\frac{\partial p}{\partial y}+\nu\left(1-\frac{B^2}{6}\left(4\left(\frac{\partial u}{\partial x}\right)^2+\left(\frac{\partial u}{\partial y}+\frac{\partial v}{\partial x}\right)^2\right)\right)^n\left(\frac{\partial^2 v}{\partial x^2}-\frac{\partial^2 u}{\partial x\partial y}\right)+\frac{2n\nu B^2}{6}$$
$$\left(1-\frac{B^2}{6}\left(4\left(\frac{\partial u}{\partial x}\right)^2+\left(\frac{\partial u}{\partial y}+\frac{\partial v}{\partial x}\right)^2\right)\right)^{n-1}$$
$$\left(8\left(\frac{\partial u}{\partial x}\right)^2\frac{\partial^2 u}{\partial x\partial y}+2\frac{\partial u}{\partial x}\left(\frac{\partial u}{\partial y}+\frac{\partial v}{\partial x}\right)\left(\frac{\partial^2 u}{\partial y^2}+\frac{\partial^2 v}{\partial x\partial y}\right)\right) \quad (2.3)$$
$$-\frac{n\nu B^2}{6}\left(1-\frac{B^2}{6}\left(4\left(\frac{\partial u}{\partial x}\right)^2+\left(\frac{\partial u}{\partial y}+\frac{\partial v}{\partial x}\right)^2\right)\right)^{n-1}$$
$$\left(8\frac{\partial u}{\partial x}\frac{\partial^2 u}{\partial x^2}\left(\frac{\partial u}{\partial y}+\frac{\partial v}{\partial x}\right)+2\frac{\partial u}{\partial x}\left(\frac{\partial u}{\partial y}+\frac{\partial v}{\partial x}\right)^2\left(\frac{\partial^2 u}{\partial x\partial y}+\frac{\partial^2 v}{\partial x^2}\right)\right),$$

$$\frac{\partial T}{\partial t}+u\frac{\partial T}{\partial x}+v\frac{\partial T}{\partial y}=\alpha\left(\frac{\partial^2 T}{\partial x^2}+\frac{\partial^2 T}{\partial y^2}\right), \quad (2.4)$$

$$\frac{\partial C}{\partial t}+u\frac{\partial C}{\partial x}+v\frac{\partial C}{\partial y}=D\left(\frac{\partial^2 C}{\partial x^2}+\frac{\partial^2 C}{\partial y^2}\right). \quad (2.5)$$

The appropriate boundary conditions corresponding to the flow problem are [13] & [27]:

$$u=U_w=\frac{ax}{1-\gamma t},\ v=0\ \ at\ y=0,$$
$$u=0,\ v=v_h=\frac{dh}{dt}=-\frac{\gamma}{2}\sqrt{\frac{\nu}{a(1-\gamma t)}}\ \ at\ y=h(t),$$
$$K\frac{\partial T}{\partial y}\Big|_{y=0}=-h_{1f}[T_f-T],\ D\frac{\partial C}{\partial y}\Big|_{y=0}=-h_{2f}[C_f-C] \quad (2.6)$$
$$at\ y=0,$$
$$K\frac{\partial T}{\partial y}\Big|_{y=h(t)}=-h_{1f}^*[T-T_h],\ D\frac{\partial C}{\partial y}\Big|_{y=h(t)}$$
$$=-h_{2f}^*[C-C_h]\ \ at\ y=h(t).$$

Here, u and v designate velocity components along axes x and y respectively. ρ denotes the fluid density, B represents the material constant of Sutterby fluid model, p considered as pressure, ν denotes the kinematics viscosity, n represents the power law index, B_o denotes the applied magnetic field, K denotes the thermal conductivity, h_{1f} and h_{2f} represents the heat and mass transport co-efficient at the lower plate respectively. T_f denotes the suspended fluid temperature, h_{1f}^* and h_{2f}^* denote the heat and mass transport co-efficient at upper plate respectively. C_f represents the suspended fluid concentration, σ denotes the electric conductivity, T denotes the fluid temperature, T_h represents the temperature of upper plate, α denotes the thermal diffusivity, C represents the fluid concentration, C_h represents the particle concentration at upper plate, D denotes the diffusion co-efficient, γ and α are the dimensional constant. In view of above analysis, we define following non dimensional quantities:

$$\eta=\frac{y}{h(t)},\ \Psi=\sqrt{\frac{a\nu}{1-\gamma t}}xf(\eta),u=U_wf'(\eta),$$
$$v=-\sqrt{\frac{a\nu}{1-\gamma t}}f(\eta),\ \theta(\eta)=\frac{T-T_h}{T_f-T_h},\ \phi(\eta)=\frac{C-C_h}{C_f-C_h}. \quad (2.7)$$

Pressure is eliminating from equations (2.2)-(2.3) and with the introduction of above said variables, the governing equations can be written as:

$$ff'''-f'f''-\frac{S_q}{2}(3f''+\eta f''')$$
$$+f^{(iv)}\left(1-\frac{\alpha_1^2}{6\delta^2}(4\delta^2(f')^2+(f'')^2)\right)^n$$
$$-\frac{n\alpha_1^2}{6\delta^2}\left(1-\frac{\alpha_1^2}{6\delta^2}(4\delta^2(f')^2+(f'')^2)\right)^{n-1}$$
$$(8\delta^2f'f''f'''+2f''(f''')^2)$$

$$+\frac{4n(n-1)\alpha_1^4}{36\delta^2}\left(1-\frac{\alpha_1^2}{6\delta^2}(4\delta^2(f')^2+(f'')^2)\right)^{n-2}$$
$$(16\delta^2(f')^2(f'')^3+4f'(f'')^3f'''-(f'')^5)$$
$$-\frac{2n\alpha_1^2}{6}\left(1-\frac{\alpha_1^2}{6\delta^2}(4\delta^2(f')^2+(f'')^2)\right)^{n-1}$$
$$(2(f'')^3+8f'f''f'''-(f'')^3)+\frac{n(n-1)\alpha_1^4}{36\delta^4}$$
$$\left(1-\frac{\alpha_1^2}{6\delta^2}(4\delta^2(f')^2+(f'')^2)\right)^{n-2} \quad (2.8)$$
$$(8\delta^2f'f''+2f''f''')\,(8\delta^2f'(f'')^2+2(f'')^2f''')$$
$$-\frac{n\alpha_1^2}{6\delta^2}\left(1-\frac{\alpha_1^2}{6\delta^2}(4\delta^2(f')^2+(f'')^2)\right)^{n-1}$$
$$(8\delta^2(f'')^3+16\delta^2f'f''f'''+4f''(f''')^2$$
$$+2(f'')^2f^{(iv)})-M^2f''=0,$$

$$\theta''-Pr\left(\frac{S_q}{2}\eta\theta'-f\theta'\right)=0, \quad (2.9)$$

$$\phi''-Sc\left(\frac{S_q}{2}\eta\phi'-f\phi'\right)=0, \quad (2.10)$$

with subjected boundary conditions:

$$f(0)=0,\ f(1)=\frac{S_q}{2},\ f'(0)=1,\ f'(1)=0,$$
$$\theta'(0)=-B_1\big(1-\theta(0)\big),\quad \theta'(1)=-B_2\theta(1), \quad (2.11)$$
$$\phi'(0)=-B_3\big(1-\phi(0)\big),\ \phi'(1)=-B_4\,\phi(1),$$

where, S_q is squeezing parameter, δ is length parameter, α_1 is non-dimensional fluid parameter, M is magnetic parameter, Pr is Prandtl number, (B_1, B_3) are lower plate thermal and solutal Biot number, (B_2, B_4) are upper plate thermal and solutal Biot numbers, Sc is Schmidt number. These parameters are given by:

$$S_q=\frac{\gamma}{a},\ \alpha_1=\frac{Ba}{1-\gamma t},\ \delta=\sqrt{\frac{\nu(1-\gamma t)}{ax^2}},\ M^2=\frac{\sigma B_o^2}{\rho a},$$
$$Pr=\frac{\nu}{\alpha},\ B_1=\frac{h_{1f}}{K}\sqrt{\frac{\nu(1-\gamma t)}{a}},\ B_2=\frac{h_{1f}^*}{K}\sqrt{\frac{\nu(1-\gamma t)}{a}}, \quad (2.12)$$
$$Sc=\frac{\nu}{D},\ B_3=\frac{h_{2f}}{D}\sqrt{\frac{\nu(1-\gamma t)}{a}},\ B_4=\frac{h_{2f}^*}{D}\sqrt{\frac{\nu(1-\gamma t)}{a}}.$$

Moreover, the plates illustrate inward movement for $S_q > 0$, and for $S_q < 0$, away movement is observed.

Defining Skin friction co-efficient, heat and mass transfer rates as follows:

$$C_f=\frac{\mu(\tau_{xy})\big|_{y=h(t)}}{\rho U_w^2},\ Nu=\frac{-xK\left(\frac{\partial T}{\partial y}\right)\Big|_{y=h(t)}}{K(T_f-T_h)},$$
$$Sh=\frac{-xD\left(\frac{\partial C}{\partial y}\right)\Big|_{y=h(t)}}{D(C_f-C_h)}, \quad (2.13)$$

the equation (2.13) in dimensionless form is:

$$(Re)^{\frac{1}{2}}C_f=f''(1)-\frac{\alpha_1^2}{6\delta^2}\left(4\big(f'(1)\big)^2f''(1)+\big(f''(1)\big)^2\right), \quad (2.14)$$
$$(Re)^{-\frac{1}{2}}Nu=-\theta'(1),\qquad (Re)^{-\frac{1}{2}}Sh=-\phi'(1).$$

3. Homotopy Analysis Solutions

Homotopic technique is a mathematical procedure which is used to develop the analytical approximation solutions of highly non-linear problems. This method facilitates us to analyze and choose the initial approximation along with linear operators which are described for considered flow problem as follows:

$$f_0(\eta)=\frac{1}{2}(2\eta-4\eta^2+3S_q\eta^2+2\eta^3-2S_q\eta^3, \quad (3.1)$$

$$\theta_0(\eta)=\frac{1}{B_1+B_2+B_1B_2}(B_1+B_1B_2-B_1B_2\eta), \quad (3.2)$$

$$\phi_0(\eta)=\frac{1}{B_3+B_4+B_3B_4}(B_3+B_3B_4-B_3B_4\eta), \quad (3.3)$$

$$\mathcal{L}_f=f^{(iv)},\ \mathcal{L}_\theta=\theta'',\ \mathcal{L}_\phi=\phi'', \quad (3.4)$$

with

$$\mathcal{L}_f(C_1+C_2\eta+C_3\eta^2+C_4\eta^3)=0,\ \mathcal{L}_\theta(C_5+C_6\eta)=0,$$
$$\mathcal{L}_\phi(C_7+C_8\eta)=0, \quad (3.5)$$

where $C_i (i = 1\text{-}8)$ are arbitrary constants.

Here, we addressed the solutions when $n = 1$ and $n = 2$ for considered flow problem.

3.1. Zeroth-order problems

Here,

$$(1-q)\mathcal{L}_f\big[\check{f}(\eta;q)-f_0(\eta)\big]=q\hbar_fN_f\big[\check{f}(\eta;q)\big],$$
$$\check{f}(0;q)=0,\ \check{f}(1;q)=\frac{S_q}{2},\ \check{f}'(0;q)=1,\ \check{f}'(1;q)=0, \quad (3.6)$$
$$(1-q)\mathcal{L}_\theta\big[\check{\theta}(\eta;q)-\theta_0(\eta)\big]=q\hbar_\theta N_\theta\big[\check{\theta}(\eta;q)\big],$$
$$\check{\theta}'(0;q)-B_1\check{\theta}(0;q)=-B_1,\ \check{\theta}'(1;q)+B_2\check{\theta}(1;q)=0, \quad (3.7)$$
$$(1-q)\mathcal{L}_\phi\big[\check{\phi}(\eta;q)-\phi_0(\eta)\big]=q\hbar_\phi N_\phi\big[\check{\phi}(\eta;q)\big],$$
$$\check{\phi}'(0;q)-B_3\check{\phi}(0;q)=-B_3,\ \check{\phi}'(1;q)+B_4\check{\phi}(1;q)=0. \quad (3.8)$$

Nonlinear operators is expressed as:

For $n = 1$

$$N_f[\check{f}(\eta;q)] = \frac{\partial^4\check{f}(\eta;q)}{\partial\eta^4} + \check{f}(\eta;q)\frac{\partial^3\check{f}(\eta;q)}{\partial\eta^3} - \frac{\partial\check{f}(\eta;q)}{\partial\eta}\frac{\partial^2\check{f}(\eta;q)}{\partial\eta^2} - \frac{S_q}{2}\left(3\frac{\partial^2\check{f}(\eta;q)}{\partial\eta^2} + \eta\frac{\partial^3\check{f}(\eta;q)}{\partial\eta^3}\right) - \frac{2\alpha_1^2}{3}\left(\frac{\partial\check{f}(\eta;q)}{\partial\eta}\right)^2\frac{\partial^4\check{f}(\eta;q)}{\partial\eta^4} - \frac{\alpha_1^2}{2\delta^2}\left(\frac{\partial^2\check{f}(\eta;q)}{\partial\eta^2}\right)^2\frac{\partial^4\check{f}(\eta;q)}{\partial\eta^4} - \frac{20\alpha_1^2}{3}\frac{\partial\check{f}(\eta;q)}{\partial\eta}\frac{\partial^2\check{f}(\eta;q)}{\partial\eta^2}\frac{\partial^3\check{f}(\eta;q)}{\partial\eta^3} - \frac{\alpha_1^2}{\delta^2}\frac{\partial^2\check{f}(\eta;q)}{\partial\eta^2}\left(\frac{\partial^3\check{f}(\eta;q)}{\partial\eta^3}\right)^2 - \frac{5\alpha_1^2}{3}\left(\frac{\partial^2\check{f}(\eta;q)}{\partial\eta^2}\right)^3 - M^2\frac{\partial^2\check{f}(\eta;q)}{\partial\eta^2}, \tag{3.9}$$

and for $n = 2$

$$N_f[\check{f}(\eta;q)] = \frac{\partial^4\check{f}(\eta;q)}{\partial\eta^4} + \check{f}(\eta;q)\frac{\partial^3\check{f}(\eta;q)}{\partial\eta^3} - \frac{\partial\check{f}(\eta;q)}{\partial\eta}\frac{\partial^2\check{f}(\eta;q)}{\partial\eta^2} - \frac{S_q}{2}\left(3\frac{\partial^2\check{f}(\eta;q)}{\partial\eta^2} + \eta\frac{\partial^3\check{f}(\eta;q)}{\partial\eta^3}\right) - \frac{4\alpha_1^2}{3}\left(\frac{\partial\check{f}(\eta;q)}{\partial\eta}\right)^2\frac{\partial^4\check{f}(\eta;q)}{\partial\eta^4} - \frac{\alpha_1^2}{\delta^2}\left(\frac{\partial^2\check{f}(\eta;q)}{\partial\eta^2}\right)^2\frac{\partial^4\check{f}(\eta;q)}{\partial\eta^4} - \frac{4\alpha_1^4}{9}\left(\frac{\partial\check{f}(\eta;q)}{\partial\eta}\right)^4\frac{\partial^4\check{f}(\eta;q)}{\partial\eta^4} + \frac{5\alpha_1^4}{36\delta^4}\left(\frac{\partial^2\check{f}(\eta;q)}{\partial\eta^2}\right)^4\frac{\partial^4\check{f}(\eta;q)}{\partial\eta^4} - \frac{40\alpha_1^2}{3}\frac{\partial\check{f}(\eta;q)}{\partial\eta}\frac{\partial^2\check{f}(\eta;q)}{\partial\eta^2}\frac{\partial^3\check{f}(\eta;q)}{\partial\eta^3} + \frac{2\alpha_1^4}{3\delta^2}\left(\frac{\partial\check{f}(\eta;q)}{\partial\eta}\right)^2\left(\frac{\partial^2\check{f}(\eta;q)}{\partial\eta^2}\right)^2\frac{\partial^4\check{f}(\eta;q)}{\partial\eta^4} - \frac{2\alpha_1^2}{\delta^2}\frac{\partial^2\check{f}(\eta;q)}{\partial\eta^2}\left(\frac{\partial^3\check{f}(\eta;q)}{\partial\eta^3}\right)^2 + \frac{80\alpha_1^4}{9}\left(\frac{\partial\check{f}(\eta;q)}{\partial\eta}\right)^3\frac{\partial^2\check{f}(\eta;q)}{\partial\eta^2}\frac{\partial^3\check{f}(\eta;q)}{\partial\eta^3} + \frac{4\alpha_1^2}{3\delta^2}\left(\frac{\partial\check{f}(\eta;q)}{\partial\eta}\right)^2\frac{\partial^2\check{f}(\eta;q)}{\partial\eta^2}\left(\frac{\partial^3\check{f}(\eta;q)}{\partial\eta^3}\right)^2 + \frac{44\alpha_1^4}{9}\frac{\partial\check{f}(\eta;q)}{\partial\eta}\left(\frac{\partial^2\check{f}(\eta;q)}{\partial\eta^2}\right)^3\frac{\partial^3\check{f}(\eta;q)}{\partial\eta^3} + \frac{5\alpha_1^4}{9\delta^4}\left(\frac{\partial^2\check{f}(\eta;q)}{\partial\eta^2}\right)^3\left(\frac{\partial^3\check{f}(\eta;q)}{\partial\eta^3}\right)^2 + \frac{28\alpha_1^4}{3}\left(\frac{\partial\check{f}(\eta;q)}{\partial\eta}\right)^2\left(\frac{\partial^2\check{f}(\eta;q)}{\partial\eta^2}\right)^3 - \frac{10\alpha_1^2}{3}\left(\frac{\partial^2\check{f}(\eta;q)}{\partial\eta^2}\right)^3 + \frac{\alpha_1^4}{3\delta^2}\left(\frac{\partial^2\check{f}(\eta;q)}{\partial\eta^2}\right)^5 - M^2\frac{\partial^2\check{f}(\eta;q)}{\partial\eta^2} \tag{3.10}$$

$$N_\theta[\check{\theta}(\eta;q)] = \frac{\partial^2\check{\theta}(\eta;q)}{\partial\eta^2} - Pr\left(\frac{S_q}{2}\eta\frac{\partial\check{\theta}(\eta;q)}{\partial\eta} - \check{f}(\eta;q)\frac{\partial\check{\theta}(\eta;q)}{\partial\eta}\right), \tag{3.11}$$

$$N_\phi[\check{\phi}(\eta;q)] = \frac{\partial^2\check{\phi}(\eta;q)}{\partial\eta^2} - Sc\left(\frac{S_q}{2}\eta\frac{\partial\check{\phi}(\eta;q)}{\partial\eta} - \check{f}(\eta;q)\frac{\partial\check{\phi}(\eta;q)}{\partial\eta}\right). \tag{3.12}$$

where embedding parameter is $q \in [0,1]$ and $\hbar_f$, $\hbar_\theta$ and $\hbar_\phi$ are auxiliary parameters which is non-zero in character.

3.2. mth-order deformation problems

Here,

$$\mathcal{L}_f[f_m(\eta) - \chi_m f_{m-1}(\eta)] = \hbar_f R_m^f(\eta), \quad f_m(0) = 0,\ f_m(1) = 0,\ f_m'(0) = 0,\ f_m'(1) = 0, \tag{3.13}$$

$$\mathcal{L}_\theta[\theta_m(\eta) - \chi_m\theta_{m-1}(\eta)] = \hbar_\theta R_m^\theta(\eta), \quad \theta_m'(0) - B_1\theta_m(0) = 0,\ \theta_m'(1) + B_2\theta_m(1) = 0, \tag{3.14}$$

$$\mathcal{L}_\phi[\phi_m(\eta) - \chi_m\phi_{m-1}(\eta)] = \hbar_f R_m^\phi(\eta), \quad \phi_m'(0) - B_3\phi_m(0) = 0,\ \phi_m'(1) + B_4\phi_m(1) = 0. \tag{3.15}$$

Nonlinear operators is expressed for $n = 1$ and $n = 2$ as follows:

For $n = 1$

$$R_m^f(\eta) = f_{m-1}^{(iv)} + \sum_{k=0}^{m-1} f_{m-1-k}f_k''' - \sum_{k=0}^{m-1} f_{m-1-k}'f_k'' - \frac{S_q}{2}(3f_{m-1}'' + \eta f_{m-1}''') - \frac{2\alpha_1^2}{3}\sum_{k=0}^{m-1}(f_{m-1-k}')^2 f_k^{(iv)} - \frac{\alpha_1^2}{2\delta^2}\sum_{k=0}^{m-1}(f_{m-1-k}'')^2 f_k^{(iv)} - \frac{20\alpha_1^2}{3}\sum_{k=0}^{m-1} f'_{m-1-k}\sum_{p=0}^{k} f_{k-p}''f_p''' - \frac{\alpha_1^2}{\delta^2}\sum_{k=0}^{m-1} f_{m-1-k}''(f_k''')^2 - \frac{5\alpha_1^2}{3}(f_{m-1}'')^3 - M^2 f_{m-1}'', \tag{3.16}$$

and for $n = 2$

$$R_m^f(\eta) = f_{m-1}^{(iv)} + \sum_{k=0}^{m-1} f_{m-1-k}f_k''' - \sum_{k=0}^{m-1} f_{m-1-k}'f_k'' - \frac{S_q}{2}(3f_{m-1}'' + \eta f_{m-1}''') - \frac{4\alpha_1^2}{3}\sum_{k=0}^{m-1}(f_{m-1-k}')^2 f_k^{(iv)} - \frac{\alpha_1^2}{\delta^2}\sum_{k=0}^{m-1}(f_{m-1-k}'')^2 f_k^{(iv)} + \frac{4\alpha_1^4}{9}\sum_{k=0}^{m-1}(f_{m-1-k}')^4 f_k^{(iv)} + \frac{5\alpha_1^4}{\delta^4}\sum_{k=0}^{m-1}(f_{m-1-k}')^4 f_k^{(iv)} - \frac{40\alpha_1^2}{3}\sum_{k=0}^{m-1} f_{m-1-k}'\sum_{p=0}^{k} f_{k-p}''f_p''' + \frac{2\alpha_1^4}{3\delta^2}\sum_{k=0}^{m-1}(f_{m-1-k}')^2\sum_{p=0}^{k}(f_{k-p}'')^2 f_p^{(iv)} - \frac{2\alpha_1^2}{\delta^2}\sum_{k=0}^{m-1} f_{m-1-k}''(f_k''')^2 + \frac{80\alpha_1^4}{9}\sum_{k=0}^{m-1}(f_{m-1-k}')^3\sum_{p=0}^{k} f_{k-p}''f_p''' + \frac{4\alpha_1^4}{3\delta^2}\sum_{k=0}^{m-1}(f_{m-1-k}')^2\sum_{p=0}^{k} f_{k-p}''(f_p''')^2 + \frac{44\alpha_1^4}{9}\sum_{k=0}^{m-1} f'_{m-1-k}\sum_{p=0}^{k}(f_{k-p}'')^3 f_p''' + \frac{5\alpha_1^4}{9\delta^4}\sum_{k=0}^{m-1}(f_{m-1-k}'')^3(f_k''')^2 + \frac{28\alpha_1^4}{3}\sum_{k=0}^{m-1}(f_{m-1-k}')^2(f_k'')^3 - \frac{10\alpha_1^2}{3}(f_{m-1}'')^3 + \frac{\alpha_1^4}{3\delta^2}(f_{m-1}'')^5 - M^2 f_{m-1}'', \tag{3.17}$$

$$R_m^{\theta}(\eta) = \theta''_{m-1} - Pr\left(\frac{S_q}{2}\eta\theta'_{m-1} - \sum_{k=0}^{m-1} f_{m-1-k}\theta'_k\right), \quad (3.18)$$

$$R_m^{\phi}(\eta) = \phi''_{m-1} - Sc\left(\frac{S_q}{2}\eta\phi'_{m-1} - \sum_{k=0}^{m-1} f_{m-1-k}\phi'_k\right), \quad (3.19)$$

$$\chi_m = \begin{cases} 0, & m \le 1 \\ 1, & m > 1' \end{cases} \quad (3.20)$$

for $q = 0$ and $q = 1$, we can write

$$\begin{aligned} &\breve{f}(\eta;0) = f_0(\eta), \quad \breve{f}(\eta;1) = f(\eta), \\ &\breve{\theta}(\eta;0) = \theta_0(\eta), \quad \breve{\theta}(\eta;1) = \theta(\eta), \\ &\breve{\phi}(\eta;0) = \phi_0(\eta), \quad \breve{\phi}(\eta;1) = \phi(\eta), \end{aligned} \quad (3.21)$$

and with the variation of q from 0 to 1, $\breve{f}(\eta;q)$, $\breve{\theta}(\eta;q)$ and $\breve{\phi}(\eta;q)$ vary from the initial solutions $f_0(\eta)$, $\theta_0(\eta)$ and $\phi_0(\eta)$ to the final solutions $f(\eta)$, $\theta(\eta)$ and $\phi(\eta)$ respectively. By Taylor series, we have

$$\begin{aligned} &\breve{f}(\eta;q) = f_0(\eta) + \sum_{m=1}^{\infty} f_m(\eta)q^m, \; f_m(\eta) = \frac{1}{m!}\frac{\partial^m \breve{f}(\eta;q)}{\partial q^m}\bigg|_{q=0}, \\ &\breve{\theta}(\eta;q) = \theta_0(\eta) + \sum_{m=1}^{\infty} \theta_m(\eta)q^m, \; \theta_m(\eta) = \frac{1}{m!}\frac{\partial^m \breve{\theta}(\eta;q)}{\partial q^m}\bigg|_{q=0}, \\ &\breve{\phi}(\eta;q) = \phi_0(\eta) + \sum_{m=1}^{\infty} \phi_m(\eta)q^m, \; \phi_m(\eta) = \frac{1}{m!}\frac{\partial^m \breve{\phi}(\eta;q)}{\partial q^m}\bigg|_{q=0}, \end{aligned} \quad (3.22)$$

we select the parameter (auxiliary) in a way that series (3.22) converge at $q = 1$. Thus, we have:

$$\begin{aligned} f(\eta) &= f_0(\eta) + \sum_{m=1}^{\infty} f_m(\eta), \\ \theta(\eta) &= \theta_0(\eta) + \sum_{m=1}^{\infty} \theta_m(\eta), \\ \phi(\eta) &= \phi_0(\eta) + \sum_{m=1}^{\infty} \phi_m(\eta), \end{aligned} \quad (3.23)$$

Generally solutions f_m, θ_m, and ϕ_m can be written in terms of special solutions (f^*_m, θ^*_m, ϕ^*_m) as

$$\begin{aligned} f_m(\eta) &= f^*_m(\eta) + C_1 + C_2\eta + C_3\eta^2 + C_4\eta^3, \\ \theta_m(\eta) &= \theta^*_m(\eta) + C_5 + C_6\eta, \\ \phi_m(\eta) &= \phi^*_m(\eta) + C_7 + C_8\eta. \end{aligned} \quad (3.24)$$

3.3. Convergence of problem

Homotopic procedure gives us immense pliability and an obvious approach to adopt and control the desire convergence of derived homotopic solutions. To determine the convergence region, $\hbar$-curves is sketched. Fig. 1(a) & 1(b) illustrate the desirable ranges for auxiliary variables $\hbar_f$, $\hbar_\theta$ and $\hbar_\phi$ such as $-1.5 \le \hbar_f \le -0.3$ and $-2.0 \le \hbar_\theta \le 0.0$ and $-2.0 \le \hbar_\phi \le 0.0$.

4. Results and Discussion

To estimate the physical attributes of the flow problem, we demonstrate the detailed impacts of diverse embedding parameters on flow velocity, temperature field and liquid concentration for specific values of power law index (i.e., $n = 1$ and $n = 2$). Figs. 2 and 3 depict the performance of squeezing parameter (S_q) on velocity field. We noticed that an increase in S_q causes enhancement in horizontal and vertical velocities. Physically, fluid experiences the force (squeezing force) when upper wall compresses towards the lower stretched sheet which helps the fluid to intensifies the deformation. Moreover, velocity field shows same enhancing behavior for $n = 1$ and $n = 2$. Fig. 4 captures the flow behavior of horizontal velocity field for dominant Sutterby fluid parameter α_1 when power law index $n = 1$. The fluid parameter α_1 predicts the decreasing effects in the interval [0 – 0.5), no variation for $\eta = 0.5$ and dominant behavior for the region (0.5 – 1.0] due to enhancement in kinetic energy of liquid. Fig. 5 depicts the analysis of Hartman number M on velocity profile which

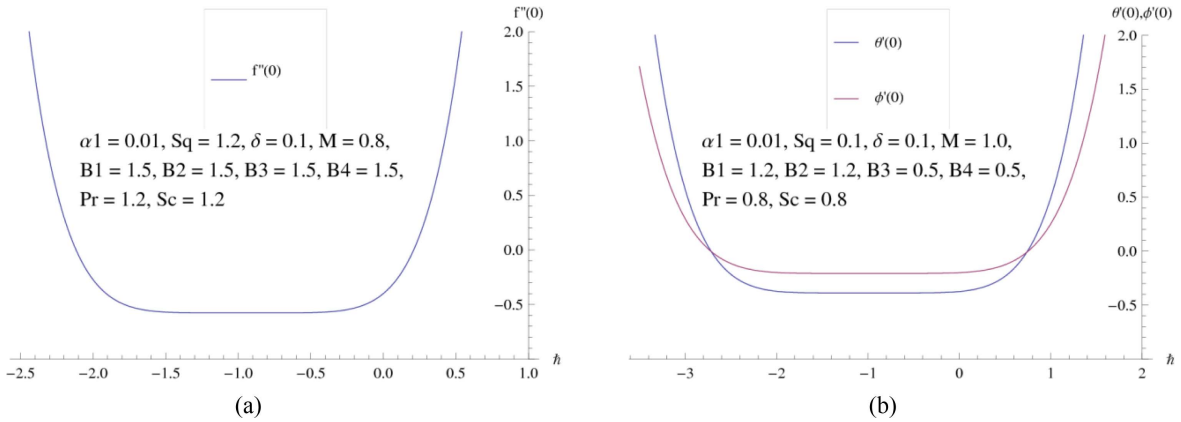

(a) (b)

Fig. 1. (Color online) (a) Convergence region for $f(\eta)$. (b) Convergence region for $\theta(\eta)$ and $\phi(\eta)$.

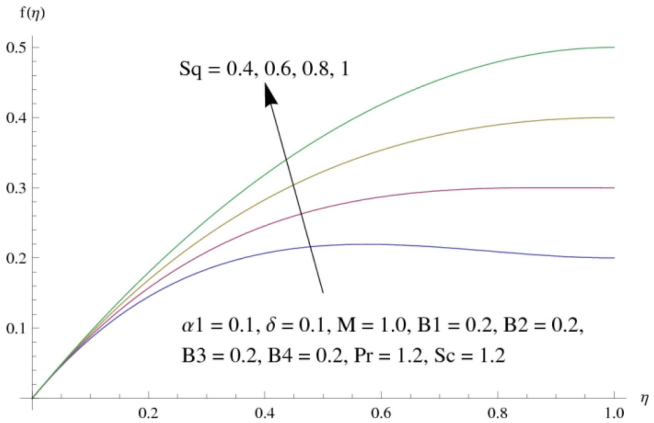

Fig. 2. (Color online) Variation of S_q on $f(\eta)$.

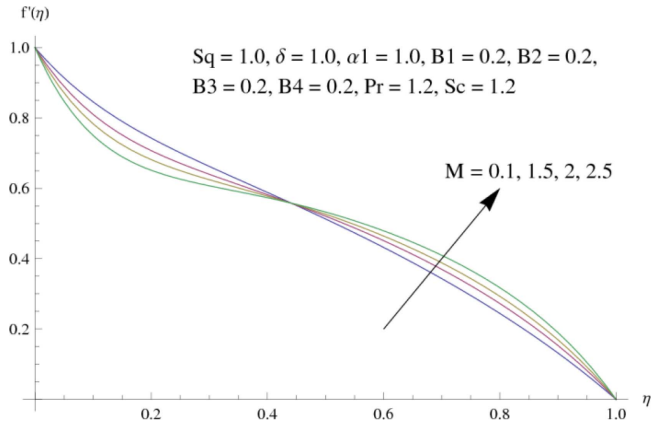

Fig. 5. (Color online) Variation of M on $f'(\eta)$.

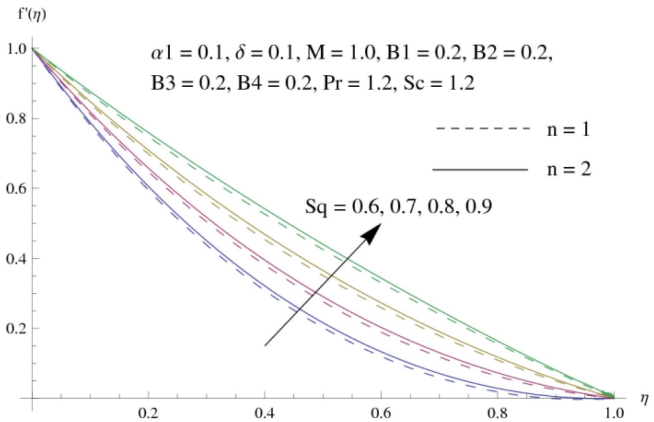

Fig. 3. (Color online) Variation of S_q on $f'(\eta)$.

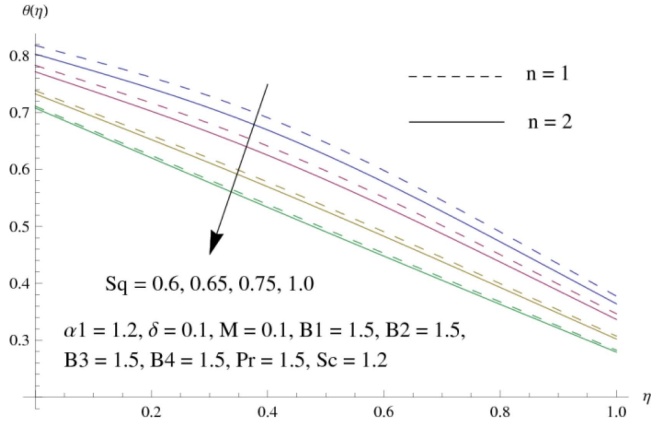

Fig. 6. (Color online) Variation of S_q on $\theta(\eta)$.

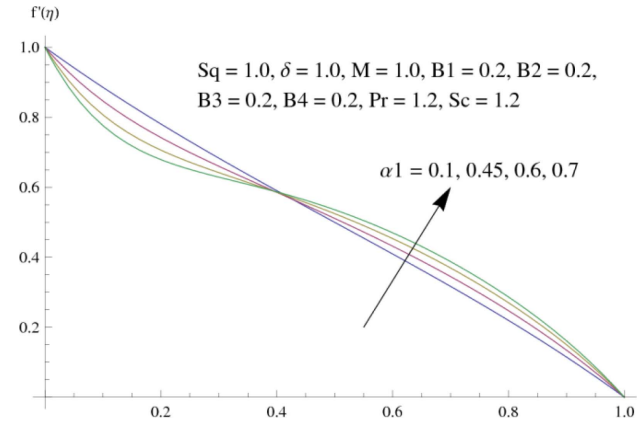

Fig. 4. (Color online) Variation of α_1 on $f'(\eta)$.

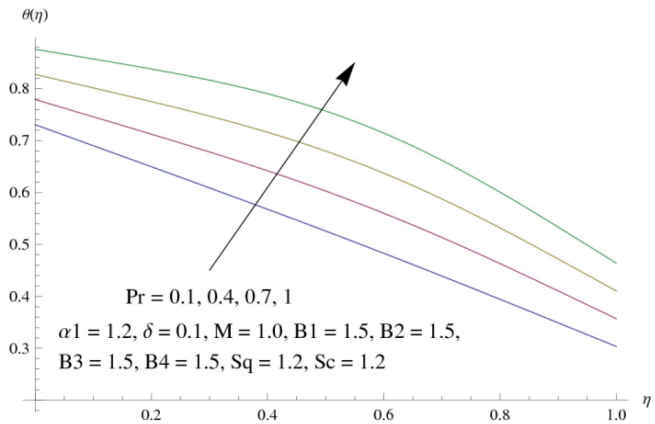

Fig. 7. (Color online) Variation of Pr on $\theta(\eta)$.

is plotted as a function of dimensionless coordinate η in the domain [0.0 – 1.0]. It is found that the velocity field reduces in the interval [0.0 – 0.5) by means of Lorentz force which is, in fact, resistive in nature. However, the opposite trend is noted in the interval (0.5 – 1.0]. Further no development in flow velocity is witnessed at $\eta = 0.5$. Fig. 6 describes the reduction in fluid's temperature for dominant squeezing parameter S_q for power law index $n = 1$ & $n = 2$. Due to decreased kinematics viscosity, the fluid temperature decays. Fig. 7 reflects the aspects of Prandtl number (Pr) on temperature field for $n = 1$. Temperature field grows up for dominant Prandtl number. For considerable Prandtl number, the thermal conductivity increases which offer extra transport of heat from heated

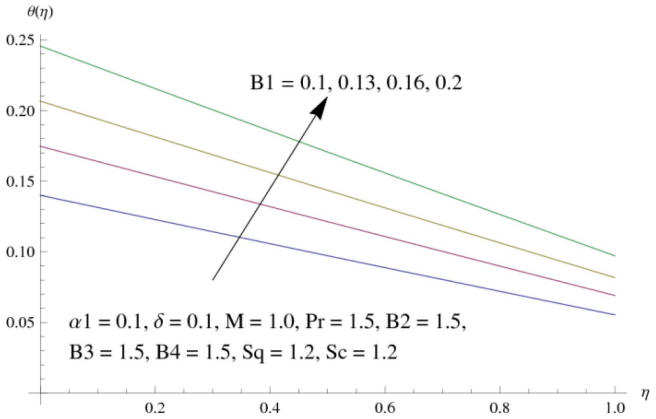

Fig. 8. (Color online) Variation of B_1 on $\theta(\eta)$.

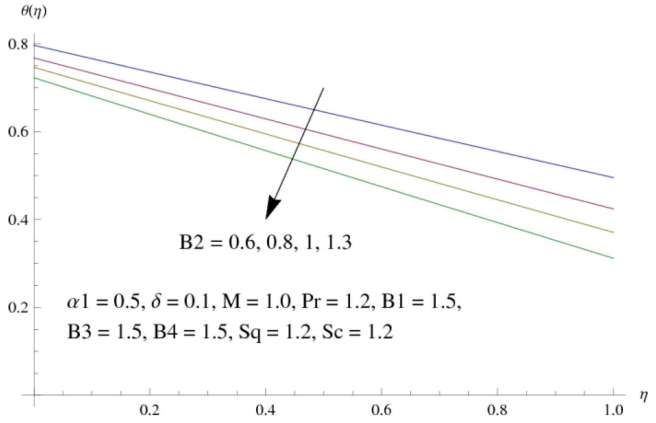

Fig. 9. (Color online) Variation of B_2 on $\theta(\eta)$.

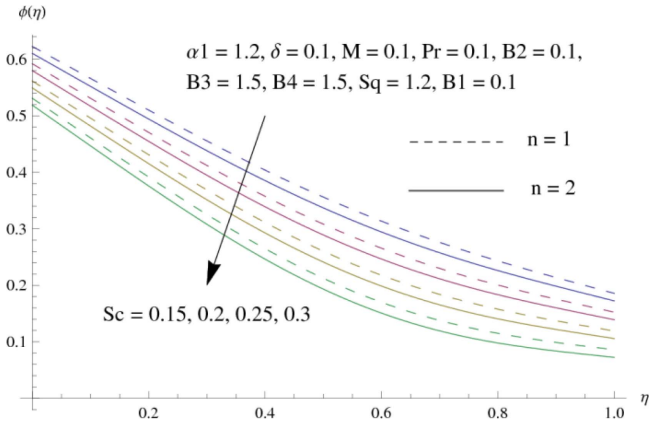

Fig. 10. (Color online) Variation of *Sc* on $\phi(\eta)$.

wall to the fluid. Therefore, fluid temperature increases. Fig. 8 illustrates that temperature is increasing function of lower plate thermal Biot number B_1 for $n = 1$. As expected for larger B_1 convective heating at lower plate increases due to which transfer of heat to fluid increases which results enhancement in fluid temperature. Fig. 9 discloses the behavior of upper plate thermal Biot number

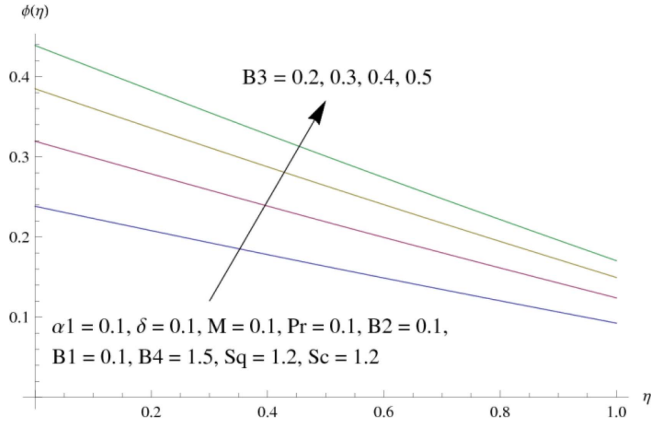

Fig. 11. (Color online) Variation of B_3 on $\phi(\eta)$.

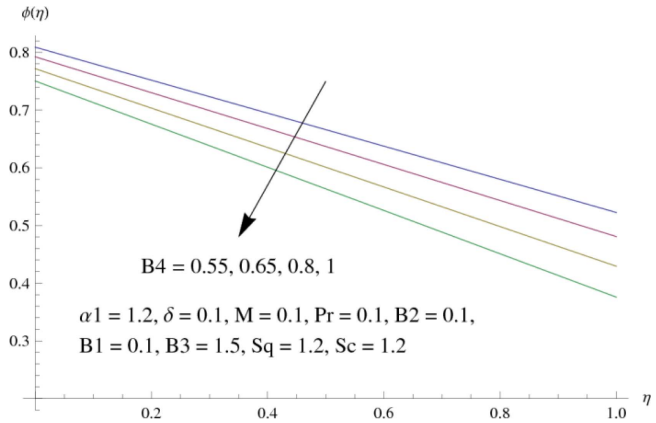

Fig. 12. (Color online) Variation of B_4 on $\phi(\eta)$.

B_2 on temperature field for $n = 1$. We noted that an enlargement in B_2 results decrement in temperature field. Since an increment in B_2 reduces the convective heating at the upper plate and so decrement in fluid temperature is noticed. Fig. 10 exhibits that concentration distribution is decreasing function of Schmidt number *Sc* for power law index $n = 1$ & $n = 2$. This is because an increment in the Schmidt number causes low diffusion rate during convection processes which is responsible for decrement in fluid concentration. Behavior of lower plate solutal Biot number B_3 on concentration field is visualized in Fig. 11. Concentration field grows up for dominant lower plate solutal Biot number B_3. In fact, more particle diffusion occurred during mass convection at the lower plate. Hence, fluid concentration enhances for $n = 1$. Fig. 12 reports the effects of upper plate solutal Biot number B_4 on concentration field. Declining behavior of concentration field is noticed for higher values of B_4. Convective mass losses at the upper plate with an increment in B_4. Therefore, fluid concentration decays for $n = 1$. Fig. 13 is plotted to see the behavior of drag force (skin friction coefficient) at upper plate. Fig illustrates that drag force

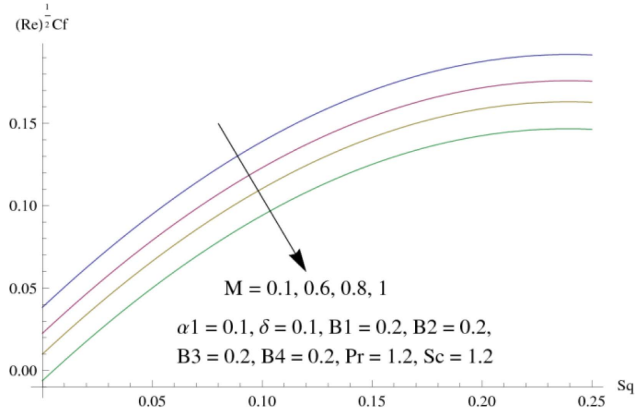

Fig. 13. (Color online) Variation of S_q & M on C_f.

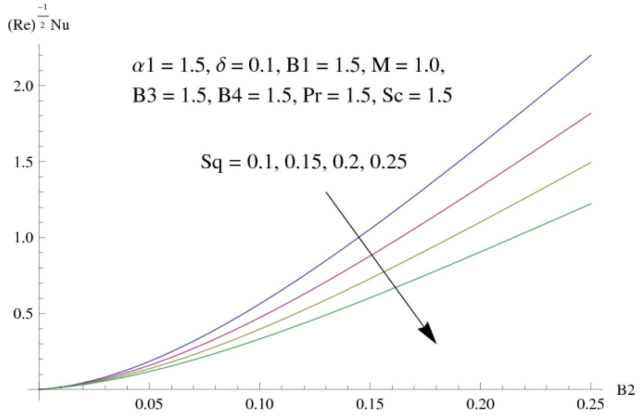

Fig. 14. (Color online) Variation of B_2 & S_q on Nu.

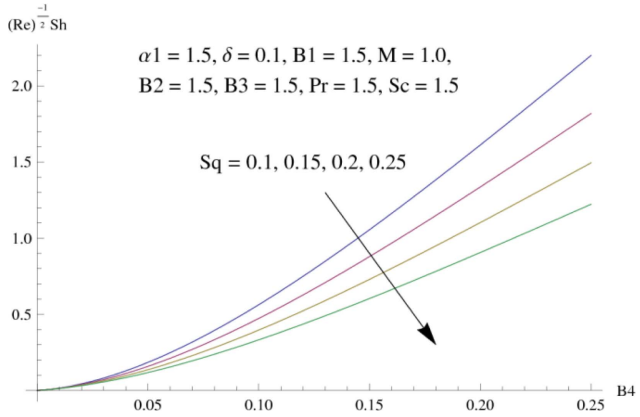

Fig. 15. (Color online) Variation of B_4 & S_q on Sh.

(skin friction coefficient) is diminishing function of Hartman number M while it is growing function of squeezing parameter S_q. Fig. 14 shows the Nusselt number Nu as increasing function of upper plate thermal Biot number B_2 while it decays for squeezing parameter S_q. Fig. 15 is graphed to notice the variation in Sherwood number Sh at upper plate. This Fig indicates that

Table 1. Comparison of skin friction co-efficient (Cf) for different values of S_q when $M = 0$, $n = 0$, and $\alpha_1 = 0$.

S_q	Muhammad *et al.* [34]	Present
	$(Re)^{1/2}C_f$	$(Re)^{1/2}C_f$
1.0	1.17039	1.17039
1.1	0.86900	0.86900
1.2	0.56585	0.56585

Sherwood number dominant for upper plate solutal Biot number B_4 whereas it decays for squeezing parameter S_q. The surface drag (or skin friction coefficient) C_f is simulated for varying values of squeezing parameter S_q with $M = 0$, $n = 0$, and $\alpha_1 = 0$. To validate the outcomes, a comparison of diverse values of drag force is made with the previous analysis Muhammad *et al.* [34] and depicted in Table 1. It is indicated that the computed results are in good agreement which reports the accuracy of the outcomes.

5. Conclusions

The present work deals with MHD flow of squeezed Sutterby fluid with convective boundary conditions. The key findings in this study are written as:

• The velocity field is found to exhibits cross flow behavior by increasing fluid parameter α_1 and Hartman number M for $n = 1$.

• The temperature and concentration distributions follow an increasing trend for enlarge lower plate thermal and solutal Biot number B_1 and B_3 correspond to power law index $n = 1$.

• A significant fall in the fluid's temperature and concentration is reported for dominant upper plate thermal and solutal Biot number B_2 and B_4 when $n = 1$.

Moreover, Implementation of MHD phenomenon diminishes the coefficient of skin friction. Therefore, beneficial work can be achieved due to less drag force under the utilization of limited energy resources. Further, squeezing mechanism causes low temperature which consequently decays the heat transfer rate. It is expected that current attempt is pertinent to the physical situation of useful stretching flows especially in energy estimation process, lubrication mechanism, food processing, magnetic polymer processing, biomedical processes, and designing of cooling/heating systems. Future investigations can be extended for more complex fluid flows such as converging flows, helical flows, nanofluid flow with single phase model. Further, three-dimensional case for squeezing flows can also be addressed.

References

[1] R. L. Batra and M. Eissa, Polym. Plast. Technol. Eng. **33**, 489 (1994).
[2] N. S. Akbar and S. Nadeem, Heat Transf. Res. **45**, 219 (2014).
[3] N. S. Akbar, International Journal of Biomathematics **8**, e1550075 (2015).
[4] T. Hayat, H. Zahir, M. Mustafa, and A. Alsaedi, Results Phys. **6**, 805 (2016).
[5] T. Hayat, A. Alsaedi, M. Rafiq, and B. Ahmad, Results Phys. **6**, 1088 (2016).
[6] E. Azhar, Z. Iqbal, and E. N. Maraj, Z. Naturforsch. A **71**, 837 (2016).
[7] T. Hayat, F. Alsaadi, M. Rafiq, and B. Ahmad, Chinese Journal of Physics **55**, 2005 (2017).
[8] T. Hayat, S. Ayub, A. Alsaedi, A. Tanveer, and B. Ahmad, Results Phys. **7**, 762 (2017).
[9] U. Shankar and N. B. Naduvinamani, Eur. Phys. J. Plus **134**, 344 (2019).
[10] T. Hayat, K. Muhammad, A. Alsaedi, and B. Ahmad, Physica Scripta, (2019), doi.org/10.1088/1402-4896/ab1c2c.
[11] N. B. Naduvinamani and U. Shankar, Sādhanā **44**, 175 (2019).
[12] N. B. Naduvinamani and U. Shankar, Journal of Central South University **26**, 1184 (2019).
[13] A. S. Eegunjobi and O. D. Makinde, Math. Probl. Eng. **2013**, e630798 (2013).
[14] S. A. Shehzad, T. Hayat, and A. Alsaedi, Bulletin of the Polish Academy of Sciences Technical Sciences **63**, 465 (2015).
[15] T. Hayat, Y. Saeed, A. Alsaedi, and S. Asad, PLoS ONE, **10**, e0133831 (2015).
[16] M. B. Ashraf, T. Hayat, A. Alsaedi, and S. A. Shahzad, Journal of Central South University **22**, 1114 (2015).
[17] K. Das, R. P. Sharma, and A. Sarkar, J. Comput. Des. Eng. **3**, 330 (2016).
[18] K. Pushpalatha, V. Sugunamma, J. V. R. Reddy, and N. Sandeep, Int. J. Adv. Res. Sci. Eng. Technol. **91**, 19 (2016).
[19] T. Hayat, M. Khan, M. Imtiaz, and A. Alsaedi, J. Mol. Liq. **225**, 569 (2017).
[20] M. Khan, M. Azam, and A. S. Alshomrani, J. Mol. Liq. **231**, 474 (2017).
[21] M. Farooq, S. Ahmad, M. Javed, and Aisha Anjum, Eur. Phys. J. Plus **133**, 63 (2018).
[22] I. Ullah, M. Waqas, T. Hayat, A. Alsaedi, and M. I. Khan, J. Therm. Anal. Calorim. **135**, 1021 (2019).
[23] X. Su and Y. Yin, J. Magn. Magn. Mater. **484**, 266 (2019).
[24] U. Shankar and N. B. Naduvinamani, Heat Transfer-Asian Research **48**, 2237 (2019).
[25] S. J. Liao, Boca Raton: Chapman and Hall, CRC Press, New York, 2003.
[26] S. J. Liao, Heidelberg: Springer and Higher Education Press, Beijing, 2012.
[27] M. Mustafa, T. Hayat, and S. Obaidat, Meccanica **47**, 1581 (2012).
[28] T. Hayat, S. Ali, M. Awais, and S. Obaidat, Progress in Computational Fluid Dynamics: An International Journal, 13 (2013), doi:10.1504/PCFD.2013.050650.
[29] T. Hayat, S. Ali, M. Awais, and M. S. Alhuthali, Applied Mathematics and Mechanics (English Edition) **36**, 61 (2015).
[30] M. Farooq, M. I. Khan, M. Waqas, T. Hayat, A. Alsaedi, and M. I. Khan, J. Mol. Liq. **221**, 1097 (2016).
[31] M. Waqas, M. Farooq, M. I. Khan, A. Alsaedi, T. Hayat, and T. Yasmeen, Int. J. Heat Mass Transf. **102**, 766 (2016).
[32] J. Zhu, D. Yang, L. Zheng, and X. Zhang, Appl. Math. Lett. **52**, 183 (2016).
[33] T. Hayat, M. I. Khan, M. Farooq, A. Alsaedi, and M. I. Khan, Int. J. Heat Mass Transf. **106**, 289 (2017).
[34] N. Muhammad, S. Nadeem, and T. Mustafa, Results Phys. **7**, 862 (2017).